Pergamon

Int. J. Heat Mass Transfer. Vol. 38, No. 16, pp. 2935–2943, 1995
Copyright © 1995 Elsevier Science Ltd
Printed in Great Britain. All rights reserved
0017–9310/95 $9.50 + 0.00

0017–9310(95)00082–8

Solidification of porous medium saturated with aqueous solution in a rectangular cell—II

K. MATSUMOTO

Department of Mechanical System Engineering, Miyazaki University, 1-1 Gakuen Kibanadai-nishi Miyazaki 889-21, Japan

M. OKADA

Department of Mechanical Engineering, Aoyama Gakuin University, 6-16-1 Chitosedai Setagaya-ku Tokyo 157, Japan

M. MURAKAMI

Toshiba Co. Ltd, 1-1-1 Shibaura Minato-ku Tokyo 105-01, Japan

and

Y. YABUSHITA

SONY Co. Ltd, 6-35 Kitashinagawa Shinagawa-ku Tokyo 141, Japan

(*Received* 22 *September* 1994 *and in final form* 7 *February* 1995)

Abstract—Three kinds of beads with different mean diameters were each packed in a rectangular cell. These packed beads were saturated with NaCl-aqueous solution and used as porous media. The solidification process of the porous medium from one of the vertical walls was studied experimentally and analytically. In the analysis, the permeability in the mushy region was expressed as the nth power function of the volume fraction of the liquid phase in the mushy region. As the results, the influences of the initial concentration of the solution and the mean diameter of beads on the solidification process were clarified.

1. INTRODUCTION

The clarification of a solidification phenomenon of a porous medium saturated with a solution is important for several engineering practices. The knowledge obtained by the clarification is useful to understand such solidification processes in a ground freezing technique where a soil containing seawater is solidified in order to support ground in a tunnel near the sea, and in a latent heat of fusion thermal energy storage system where a binary phase change material containing a high thermal conductivity material to enhance the heat transfer is solidified.

For the solidification of the solution, an analytical study taking account of the effects of mass diffusion and natural convection due to temperature and concentration gradients (so-called double-diffusive convection) was done by Incropera *et al.* [1]. For the solidification of a porous medium saturated with liquid, a study using pure water as the liquid was reported by one of the authors [7]. Recently, a few studies on the solidification of the porous medium saturated with a binary solution have been reported by Cao and Poulikakos [2] and Chio and Viskanta [3, 4]. However, these studies were done by experiment only or by an analysis where mass diffusion and natural convection were neglected. The effects of mass diffusion and the double-diffusive convection, which are important factors governing the solidification process, have not been sufficiently discussed. Although the double-diffusive convection is strongly affected by permeability in a mushy region containing both the liquid and solidified phases, physical parameters governing the permeability are still barely known.

The authors offer a simple transient measurement method of the permeability. In the method it is considered that the solute distribution in the porous medium was uniform and was kept at the state before solidification. Values of the permeabilities in the mushy region were measured, varying the initial concentration of the solution and the mean diameter and the material of beads which composed the porous medium. It was found that in the case of a porous medium packed by glass beads with 2.56 mm mean diameter and saturated with the initial concentration of solution $C_i = 10$ wt%, the permeability was

NOMENCLATURE

a	thermal diffusivity [$m^2\ s^{-1}$]
c	specific heat [J $(kg\ K)^{-1}$]
$(c\rho)$	heat capacity [J $(m^3\ K)^{-1}$]
$(c\rho)_e$	effective heat capacity [J $(m^3\ K)^{-1}$]
$(c\rho)_e^*$	$(c\rho)_e/(c\rho)_L$
$(c\rho)_L$	heat capacity of solution [J $(m^3\ K)^{-1}$]
C	concentration [wt%]
C_v	mass concentration, where $\{C_v = (0.02379C^2 + 7.051C + 999.5)C/100\}$
C_{vC}	saturated mass concentration at T_C [$kg\ m^{-3}$]
C_{vi}	initial mass concentration [$kg\ m^{-3}$]
C_{vW}	saturated mass concentration at T_W [$kg\ m^{-3}$]
D	mass diffusivity [$m^2\ s^{-1}$]
Fo	Fourier number $\{(t/h^2)\ \lambda_{eL}/(c\rho)_L\}$
g	gravitational acceleration [$m\ s^{-2}$]
h	height of cell [m]
Δh	latent heat of fusion [J kg^{-1}]
L	width of cell [m]
Le	Lewis number $\{[\lambda_{eL}/(c\rho)_L]\ (1/D)\}$
k	permeability [m^2]
k_0	permeability before solidification [m^2]
k^*	k/k_0
n	exponent of equation (1)
Ra_C	Rayleigh number based on concentration difference $\{g\beta_C(C_{vW} - C_{vi})h^3/[\nu(\lambda_{eL}/(c\rho)_L)]\ (k_0/h^2)\}$
Ra_T	Rayleigh number based on temperature difference $\{g\beta_T(T_{iL} - T_W)h^3/[\nu(\lambda_{eL}/(c\rho)_L)]\ (k_0/h^2)\}$
Ste	Stefan number $\{(c\rho)_L(T_{iL} - T_W)/(\rho_S\Delta h)\}$
t	time [s]
T	temperature [°C]
T_B	brine temperature at the cold wall [°C]
T_C	temperature of the cold wall [°C]
T_h	temperature of the hot wall [°C]
T_{iL}	solidification temperature corresponding to initial concentration [°C]
T_W	temperature of the cold wall after T_C becomes constant [°C]
u	apparent velocity in the x-direction [$m\ s^{-1}$]
U	$[(c\rho)_L/\lambda_{eL}]\ (uh)$
v	apparent velocity in the y-direction [$m\ s^{-1}$]
V	$[(c\rho)_L/\lambda_{eL}]\ (vh)$
x, y	Cartesian coordinates [m]
X	x/h
Y	y/h.

Greek symbols

α	$C_{vi}/(C_{vW} - C_{vi})$
β_C	volumetric expansion coefficient based on concentration variation [$(kg\ m^{-3})^{-1}$]
β_T	volumetric expansion coefficient based on temperature variation [K^{-1}]
θ	$(T - T_{iL})/(T_{iL} - T_W)$
θ_C	$(T_C - T_{iL})/(T_{iL} - T_W)$
θ_{ET}	$(T_{ET} - T_{iL})/(T_{iL} - T_W)$
θ_h	$(T_h - T_{iL})/(T_{iL} - T_W)$
θ_i	$(T_i - T_{iL})/(T_{iL} - T_W)$
λ_e	effective thermal conductivity [W $(m\ K)^{-1}$]
λ_{eL}	effective thermal conductivity of porous medium composed of liquid phase and beads [W $(m\ K)^{-1}$]
λ_{eS}	effective thermal conductivity of porous medium composed of solid phase and beads [W $(m\ K)^{-1}$]
λ_e^*	λ_e/λ_{eL}
μ	coefficient of viscosity [$kg\ (m\ s)^{-1}$]
ν	kinetic viscosity [$m^2\ s^{-1}$]
π	$(C_v - C_{vi})/(C_{vW} - C_{vi})$
π_C	$(C_{vC} - C_{vi})/(C_{vW} - C_{vi})$
π_{ET}	$(C_{vET} - C_{vi})/(C_{vW} - C_{vi})$
ρ	density [$kg\ m^{-3}$]
ψ	stream function [$m^2\ s^{-1}$]
Ψ	$[(c\rho)_L/\lambda_{eL}]\ \psi$
Φ	porosity $\{\Phi = (V_0 - V_1)/V_0\}$
χ	volume fraction of liquid phase when the porous medium is in a mushy state, or volume fraction of liquid phase and eutectic solid when the porous medium is in a eutectic state $\{\chi = (V_0 - V_1 - V_2)/V_0\}$
(χ/Φ)	ratio of volume fraction of liquid phase in mushy region to porosity
ω	eutectic fraction $\{\omega = V_3/V_0\}$
$(\chi - \omega)$	volume fraction of liquid phase $\{(\chi - \omega) = V_4/V_0\}$ where V_0 = control volume in porous medium $\{V_0 = V_1 + V_2 + V_3 + V_4\}$, V_1 = volume of beads in the control volume, V_2 = volume of pure ice in the control volume, V_3 = volume of eutectic solid in the control volume, V_4 = volume of liquid phase in the control volume.

Subscripts

ET	eutectic point
i	initial value
L	liquid phase (solution)
S	solid phase (ice or eutectic solid).

approximately proportional to 16th power of the volume fraction of the liquid phase in the mushy region [8].

In the previous report [5], several kinds of beads, each packed in a rectangular cell, were used as the porous medium, and the porous medium saturated with NaCl-aqueous solution of 10 or 3 wt% initial concentration was solidified from one of the vertical walls of the cell. Though the solute flowed in the mushy region and the distribution of the volume fraction of the liquid phase and the distribution of concentration in the liquid phase were not uniform, it was shown that the local permeability in the mushy region was able to be expressed as the function of the local volume fraction of the liquid phase χ, namely, as the following equation:

$$(k/k_0) = (\chi/\Phi)^n \tag{1}$$

where k_0 and Φ are described in the Nomenclature.

This equation was the same function that was obtained by the mesurement of the permeability in ref. [8]. It was shown that the exponent n of equation (1), which was considered to be dependent on the solidification process, did not depend on the bead material. Besides, the characteristics of the solidification process and the effects of the bead properties, especially the thermal conductivity of bead, on the process were clarified by an experiment and a numerical analysis.

In the present paper, the experiment and analysis in the same manner as the previous report [5] are done, varying the bead material, the mean diameter of beads and the initial concentration of the solution. The results of the distributions of temperature, concentration, stream function, the position of the freezing front and the ratio of the volume fraction of the liquid phase to the porosity (χ/Φ) are obtained. From these results the influences of the mean diameter of beads and the initial concentration of the solution on the solidification process are clarified.

2. ANALYSIS

2.1. *Analytical model*

The analytical model is shown in Fig. 1. Beads packed in a rectangular cell are treated as a porous medium. The height and width of the cell are h and L, respectively. The temperature of the left vertical wall (cold wall) is T_C and that of the right vertical wall (hot wall) is T_h ($T_h > T_C$), and both the horizontal walls of the cell are insulated. The pores between the beads are filled with the NaCl-aqueous solution of predetermined initial concentration. Under the condition that the initial temperature distribution of the porous medium is uniform, the porous medium is solidified from the cold wall. Then a solid region, a mushy region and a liquid region appear in the porous medium, as shown in Fig. 1. In the analysis the double diffusive convection in both the mushy region and the liquid region and the mass diffusion are taken into account and applied to this model.

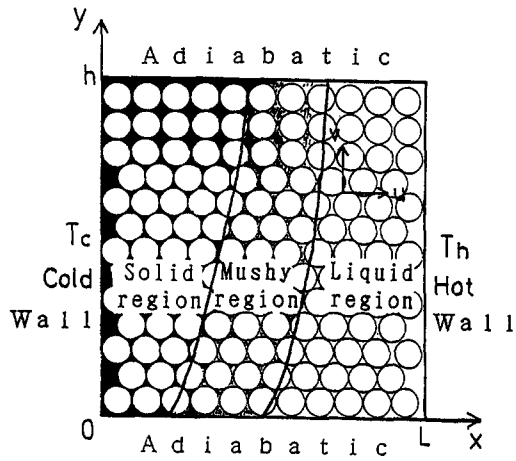

Fig. 1. Analytical model.

2.2. *Fundamental equations*

The main assumptions for the analysis are as follows:

(1) The analytical model is two-dimensional in x–y coordinates.

(2) The flow in the porous medium is governed by Darcy's law.

(3) Boussinesq approximation is valid.

(4) Effective thermal properties in the mushy region and at the eutectic point can be expressed as equation (2).

(5) Local phase equilibrium in the mushy region is valid.

(6) The relationship between the solidification temperature and concentration of NaCl-solution can be approximated by a straight line for the full range of this calculation.

(7) Latent heat of fusion of ice in an aqueous solution is constant.

(8) The properties of a eutectic solid are equal to those of pure ice.

(9) Mass diffusivity is constant.

(10) Volume expansion due to phase change is negligible.

The assumptions (7) and (8) should be discussed more, however these assumptions are adopted in the present analysis because the applicable data are not known.

The nondimensional governing equations, and the nondimensional initial and boundary conditions are given as follows:

effective values of thermal properties:

$$A_e = \frac{\chi-\omega}{\Phi}A_{eL} + \left(1-\frac{\chi-\omega}{\Phi}\right)A_{eS} \tag{2}$$

where $A = \lambda$, or $(c\rho)$

energy equation

$$(c\rho)_e^* \frac{\partial\theta}{\partial Fo} + \frac{\partial U\theta}{\partial X} + \frac{\partial V\theta}{\partial Y} = \frac{\partial}{\partial X}\left(\lambda_e^* \frac{\partial\theta}{\partial X}\right) + \frac{\partial}{\partial Y}\left(\lambda_e^* \frac{\partial\theta}{\partial Y}\right) - \frac{1}{Ste}\frac{\partial(\chi-\omega)}{\partial Fo} \quad (3)$$

diffusion equation

$$\chi\frac{\partial\pi}{\partial Fo} + \frac{\partial U\pi}{\partial X} + \frac{\partial V\pi}{\partial Y} = \frac{1}{Le}\left[\frac{\partial}{\partial X}\left((\chi-\omega)\frac{\partial\pi}{\partial X}\right) + \frac{\partial}{\partial Y}\left((\chi-\omega)\frac{\partial\pi}{\partial Y}\right)\right] - (\pi+\alpha)\frac{\partial\chi}{\partial Fo} \quad (4)$$

momentum equation

$$\frac{\partial}{\partial X}\left(\frac{1}{k^*}\frac{\partial\Psi}{\partial X}\right) + \frac{\partial}{\partial Y}\left(\frac{1}{k^*}\frac{\partial\Psi}{\partial Y}\right) = -Ra_T\frac{\partial\theta}{\partial X} - Ra_C\frac{\partial\pi}{\partial X} \quad (5)$$

velocities

$$U = \frac{\partial\Psi}{\partial Y} \quad (6)$$

$$V = -\frac{\partial\Psi}{\partial X} \quad (7)$$

$$[\text{I.C.}]\ \theta = \theta_i \quad \pi = U = V = \Psi = 0 \quad (8)$$

$$[\text{B.C.}]\ \theta = \theta_C \quad \pi = \pi_C\ [\text{when } \theta_C > \theta_{ET}] \text{ or } \pi = \pi_{ET}\ [\text{when } \theta_C \leqslant \theta_{ET}]\ (X = 0)$$
$$\Psi = 0\ (\text{at solid–mush interface}) \quad (9)$$

$$\theta = \theta_h \quad \frac{\partial\pi}{\partial X} = U = \Psi = 0 (X = L/h) \quad (10)$$

$$\frac{\partial\theta}{\partial Y} = \frac{\partial\pi}{\partial Y} = V = \Psi = 0 (Y = 0 \quad Y = 1) \quad (11)$$

where the governing equations are: in the liquid region, equations (1)–(7) with $\chi = \Phi$ and $\omega = 0$; in the mushy region, equations (1)–(7) with $\pi = -\theta$, $0 < \chi < \Phi$ and $\omega = 0$; at the eutectic point, equations (1)–(7) with $\pi = \pi_{ET}$, $\theta = \theta_{ET}$, and in the solid region, equations (2), (3) with $U = V = 0$ and $\chi = \omega$.

2.3. *Evaluation of permeability in mushy region*

As the validity of evaluation of the permeability in the mushy region was fully discussed in the previous report [5], in the present paper we briefly refer to the base of the validity.

The permeability in the mushy region is expressed as equation (1) and the exponent n of equation (1) is determined by comparing the analytical results for the concentration in the liquid region with the experimental ones in the period in which the rate of the concentration rise in the liquid region becomes stable after the initial stage of the solidification. Figure 2 shows the relationships between (k/k_0) and (χ/Φ), where the values of the exponent n were obtained for various values of initial concentration C_i and mean diameter of beads D_b. From Fig. 2, it is found that the value of (k/k_0) varies rapidly in the range from $(\chi/\Phi) = 0.5$–0.7. The exponent n shows a tendency to increase with the increase of the value of C_i. The reason is considered because the size of ice crystal formed between beads decreases with the increase of C_i. We do not have enough data to discuss quantitatively the relationships between the exponent n and D_b, but it is found that the value of the permeability k decreases with the decrease of the value of D_b. As mentioned in the Introduction, it was shown in the previous paper [5] that the value of n hardly depends on the bead material.

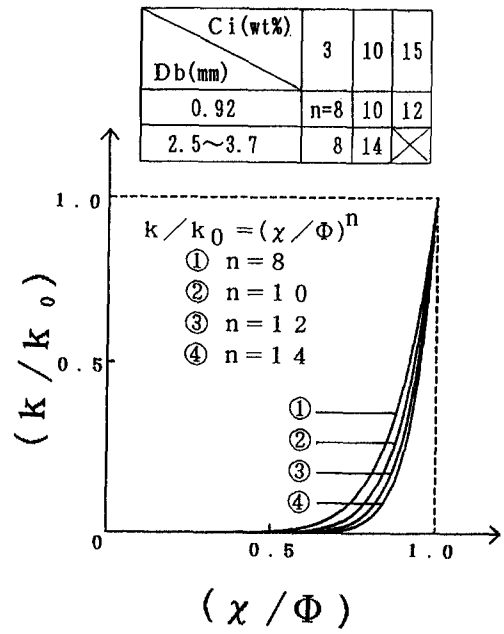

Fig. 2. Relationship between permeability and volume fraction of liquid phase in mushy region.

As clarified from the result that the exponent n is also the function of the initial concentration (see Fig. 2), in the strict sense the permeability in the mushy region is not the function of only the volume fraction of liquid phase χ, but it may also be affected by the local concentration in the solidification process. However, the present analysis where the permeability is the function only of χ will be able to simulate the fundamental phenomenon of the solidification process and it will be shown in the following result that this treatment is valid.

Concentrations measured by the experiment and obtained by the analysis with various values of the exponent n are shown in Fig. 3, in the case of vinyl chloride beads with 3.76 mm mean diameter, $T_i = T_h = 0°C$, $T_B = -30°C$, and $C_i = 10$ wt%. The concentrations are values at the point ($x = 90$ mm,

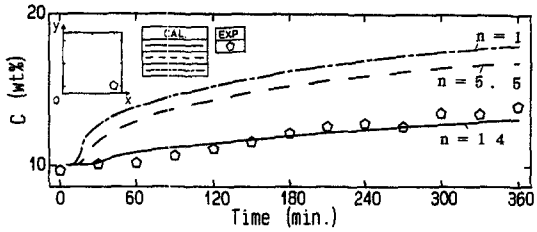

Fig. 3. Comparison of analytical result with experimental one in the case of vinyl chloride beads in order to check the validity of the present analysis. (x, y) ○ (90, 10 mm); $D_b = 3.76$mm; $C_i = 10$ wt%; $T_i = T_h = 0°C$; $T_B = -30°C$; $\Phi = 0.362$; $k_0 = 7.04 \times 10^{-9}$ m^2; $Ra_C = -4000$; $Ra_T = 29.4$.

$y = 10$ mm) where the concentration rise is the largest among the measurement points for the concentration of the liquid region. In Fig. 3, the symbol represents the experimental result and three kinds of lines represent the analytical results. The chain line corresponds to the simplest case of equation (1), where the exponent n of equation (1) is equal to 1, the dashed line corresponds to the case where n is decided on the basis of Rumpf and Gupte's report [6] ($n = 5.5$) and the solid line corresponds to the present paper's case ($n = 14$). Though both the cases of $n = 1$ and $n = 5.5$ have large differences between the analytical and experimental results, the analytical result for the case of $n = 14$ agrees well with the experimental ones. Therefore, it can be said that the expression of the permeability in the mushy region is valid.

3. EXPERIMENT

In the experiment, glass, vinyl chloride and steel are chosen as the bead materials composing the porous media because of their thermal conductivity.

The experimental apparatus is shown in Fig. 4. As the detail for the measurement is decribed in the previous report [5], in the present paper we will only briefly explain the measurements of temperature and concentration and the experimental procedure.

The temperature is measured by type T thermocouples of 0.2 mm in diameter. Especially, for the measurement in the porous medium, a probe made of thermocouples inserted into a stainless tube with 0.6 mm inner and 0.8 mm outer diameters is used; 55 temperature measurement points were arranged in a staggered configuration. About 0.25 ml of solution in the liquid region is sucked up by a syringe, and the local concentration of the solution in the liquid region is measured by a concentration-meter (salt analyzer based on coulometric titration). As it was difficult to suck up the solution in the mushy region, when the front of mushy region reached the measuring point of the concentration, the measurement of concentration was ended.

Spherical beads are packed in the rectangular cell and the packed bed is used as a porous medium. The porous medium is saturated with NaCl-aqueous solution having predetermined concentration. When the temperature distribution in the porous medium reaches within $\pm 0.5°C$ of the predetermined temperature (0°C), the solidification of the porous medium from one of the vertical walls is initiated by letting the lower temperature brine flow behind the left vertical wall.

The above experimental procedure is repeated, varying the bead material, the mean diameter of beads and the initial concentration of the solution.

4. COMPARISON OF ANALYTICAL RESULTS WITH EXPERIMENTAL ONES AND DISCUSSION

The typical results, where $T_i = T_h = 0°C$ and $T_B = -30°C$, will be shown in the following discussion. In the analysis, the experimental results of temperature on the cold and hot walls are used as the boundary conditions. Measured values of Φ and k_0 are also used. For the exponent n of equation (1), the values shown in Fig. 2 are used.

The relationship between temperature and time for the case of $C_i = 10$ wt% and the glass beads with $D_b = 2.56$ mm is shown in Fig. 5. In Fig. 5, the symbols and lines show the experimental and analytical results, respectively. As is evident from Fig. 5, there is a temperature difference between the upper and lower parts of the cell due to a natural convection.

Isotherms in the cases where the initial concentration of solution C_i and mean diameter of beads

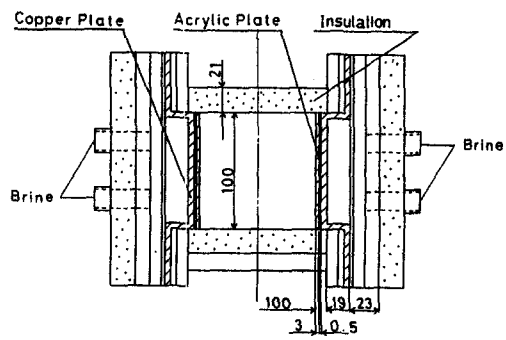

Fig. 4. Experimental apparatus.

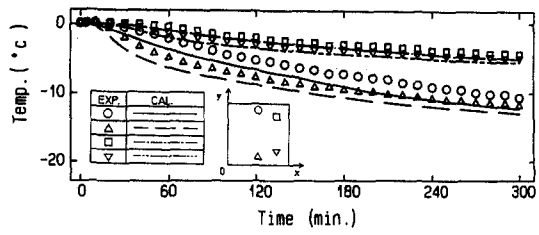

Fig. 5. Relationship between temperature and time in the case of glass beads. (x, y) △ (50, 10 mm), ○ (50, 90), ▽ (80, 20), □ (80, 80); $D_b = 2.56$ mm; $C_i = 10$ wt%; $T_i = T_h = 0°C$; $T_B = -30°C$; $\Phi = 0.380$; $k_0 = 5.00 \times 10^{-9}$ m^2; $Ra_C = -1030$; $Ra_T = 7.58$.

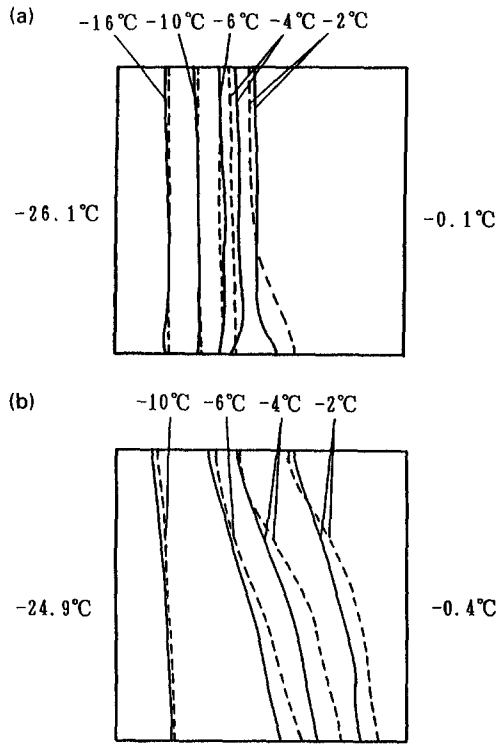

Fig. 6. Temperature distribution in the case of vinyl chloride beads. (—) Experimental results; (- - -) analytical results. $t = 120$ min; $D_b = 3.76$ mm; $T_i = T_h = 0°C$; $T_B = -30°C$; $\Phi = 0.362$; $k_0 = 7.04 \times 10^{-9}$ m^2. (a) $C_i = 3$ wt% ($Ra_C = -5550$, $Ra_T = 36.9$); (b) $C_i = 10$ wt% ($Ra_C = -4000$, $Ra_T = 29.4$).

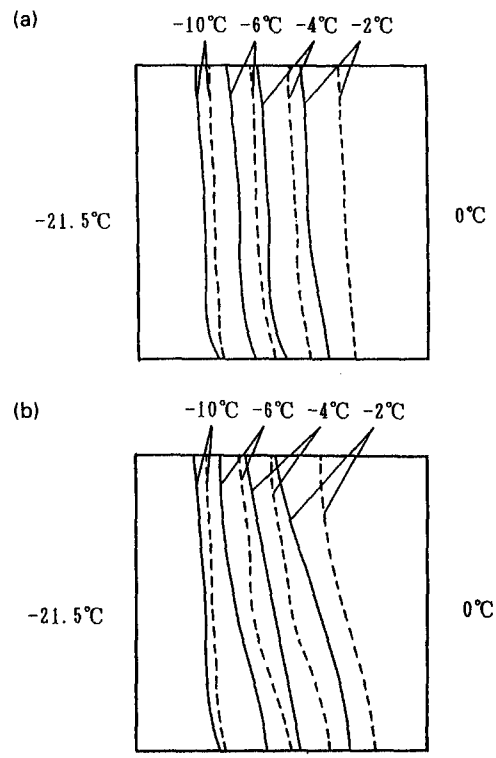

Fig. 7. Temperature distribution in the case of glass beads. (—) Experimental results; (- - -) analytical results. $t = 60$ min; $C_i = 10$ wt%; $T_i = T_h = 0°C$; $T_B = -30°C$. (a) $D_b = 0.92$ mm ($Ra_C = -97.7$, $Ra_T = 0.717$, $\Phi = 0.380$, $k_0 = 4.73 \times 10^{-10}$ m^2); (b) $D_b = 2.56$ mm ($Ra_c = -1030$, $Ra_T = 7.58$, $\Phi = 0.380$, $k_0 = 5.00 \times 10^{-9}$ m^2).

D_b vary are given in Figs. 6 and 7, respectively. The isotherms are calculated by means of the interpolation of the experimental and analytical results. In both figures, the solid and dashed lines represent the experimental and analytical results, respectively. Figure 6 shows the isotherms at $t = 120$ min for the vinyl chloride beads with $D_b = 3.76$ mm, and Fig. 7 at $t = 60$ min for $C_i = 10$ wt% and the glass beads, where $t = 60$ min is in the initial stage of the solidification process. From comparison of Fig. 6a with b, it is found that the temperature difference between the upper and lower parts of the cell in the case of the lower concentration of the solution is smaller than that in the case of the higher concentration. Because the solidification temperature of the solution rises with the decrease of the initial concentration of the solution, so the convection is suppressed due to decrease of the temperature difference in the x-direction of the liquid region and also the temperature difference in the y-direction becomes small. From Fig. 7a and b, it is found that the natural convection is suppressed with the decrease of D_b because the permeability decreases with the decrease of D_b. Therefore, the isotherms in the case of Fig. 7a are nearly parallel to the cold wall compared with those in the case of Fig. 7b. As shown in Fig. 7, particularly, in the initial stage of the solidification process the difference between the experimental and analytical results becomes larger. This is probably because the permeability in the mushy region is expressed as equation (1) and the exponent n of equation (1) is determined from the experimental results for concentration of the liquid region in the final stage of the solidification. Both the results agree gradually with each other as time passes and, finally, agree well with each other.

The relationship between the concentration and time in the case of the vinyl chloride beads with $D_b = 3.76$ mm and $C_i = 3$ wt% is shown in Fig. 8. In Fig. 8, the symbols and the lines show the experimental and analytical results, respectively. As mentioned in the discussion for Fig. 7, there remain some problems for the evaluation of the permeability in the mushy region, that is, in addition to (χ/Φ), there are some other factors governing (k/k_0). But in the results as shown in Figs. 5–8, the differences between the analytical and experimental results are small, so it can be considered that the present analysis simulates approximately the whole solidification process. In case (1) of Fig. 8, the measurement values at $x = 50$ mm after 120 min are not indicated, because, as stated in Section 3, the concentration in the mushy region was not measured. The solid line corresponding to the analytical result for case (1) of Fig. 8 rises rapidly from $t \fallingdotseq 140$ min because the front of the mushy

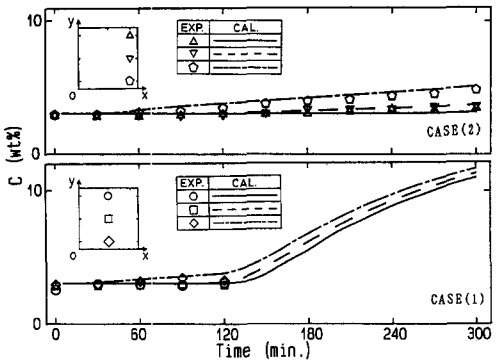

Fig. 8. Relationship between concentration and time in the case of vinyl chloride beads. Case (1) (x, y) ◇ (50, 10 mm), □ (50, 50), ○ (50, 90); case (2) (x, y) ✪ (90, 10 mm), ▽ (90, 50), △ (90, 90). $D_b = 3.76$ mm, $C_i = 3$ wt%, $T_i = T_h = 0°C$, $T_B = -30°C$, $\Phi = 0.362$, $k_0 = 7.04 \times 10^{-9}$ m^2, $Ra_C = -5550$, $Ra_T = 36.9$.

region reaches the measurement point of concentration at that time. From the comparison of symbol △ ($x = 90$ mm, $y = 90$ mm) in case (2) of Fig. 8 with symbol ✪ ($x = 90$ mm, $y = 10$ mm) in case (2), a certain concentration difference in the y-direction arises in the liquid region.

In the case of the vinyl chloride beads with $D_b = 3.76$ mm, the analytical results for time dependency of the position of the freezing front (mushy–liquid) are shown in Fig. 9. The dashed and solid lines in Fig. 9 correspond to the cases of $C_i = 3$ and 10 wt%, respectively. As is evident from Fig. 9, the growth rate of the freezing front increases with the decrease of C_i because the temperature gradients in the x-direction in the solid and mushy regions increase due to a rise of the solidification temperature with the decrease of C_i. The results calculated with different D_b, which are omitted here, show that the growth rate of the freezing front increases with the decrease of D_b because the convection is suppressed due to decrease of the permeability with the decrease of D_b.

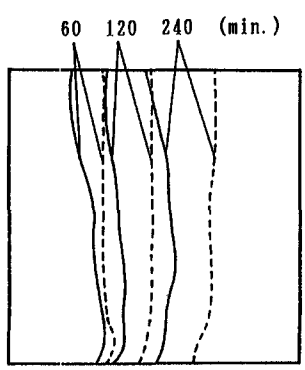

Fig. 9. Analytical results for time dependency of position of freezing front (mushy–liquid) in the case of vinyl chloride beads. $D_b = 3.76$ mm, $T_i = T_h = 0°C$, $T_B = -30°C$, $\Phi = 0.362$, $k_0 = 7.04 \times 10^{-9}$ m^2. (---) $C_i = 3$ wt% ($Ra_C = -5550$, $Ra_T = 36.9$); (—) $C_i = 10$ wt% ($Ra_C = -4000$, $Ra_T = 29.4$).

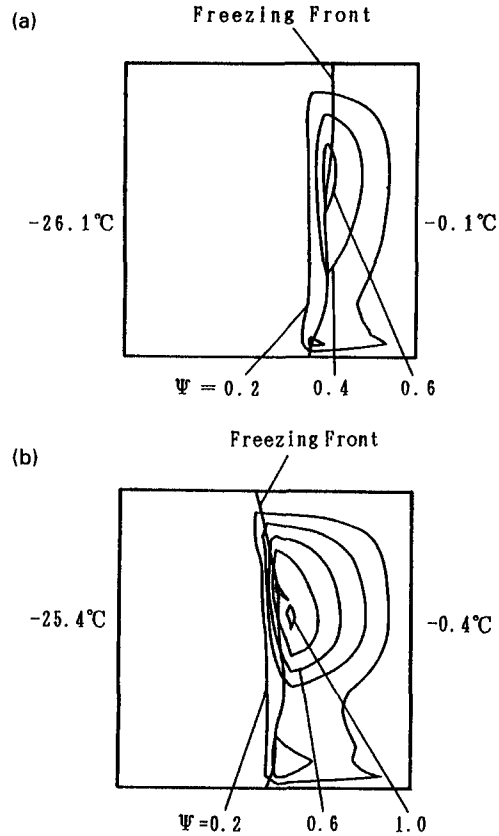

Fig. 10. Analytical results for distribution of stream function in the case of vinyl chloride beads. $t = 240$ min, $D_b = 3.76$ mm, $T_i = T_h = 0°C$, $T_B = -30°C$, $\Phi = 0.362$, $k_0 = 7.04 \times 10^{-9}$ m^2. Interval of stream-line = 0.2. (a) $C_i = 3$ wt% ($Ra_C = -5550$, $Ra_T = 36.9$); (b) $C_i = 10$ wt% ($Ra_C = -4000$, $Ra_T = 29.4$).

In the cases of the vinyl chloride beads with $D_b = 3.76$ mm, the analytical results for the non-dimensional stream function Ψ in the mushy and liquid regions at $t = 240$ min are shown in Fig. 10. The cases of $C_i = 3$ wt% and 10 wt% correspond to Fig. 10a and b, respectively. The discussion for time dependency of Ψ is omitted in the present paper because in the previous report [5] we had already done it. From Fig. 10a and b, the maximum value of Ψ in the case of $C_i = 3$ wt% is smaller than that in the case of $C_i = 10$ wt%. The natural convection in the liquid region is suppressed with the decrease of C_i because the temperature difference between the solidification temperature and the hot wall temperature decreases with the decrease of C_i. In addition, the convections in the mushy and liquid regions are suppressed with the decrease of D_b because the permeability decreases with the decrease of D_b (not shown here).

The analytical results for distributions of the concentration in the liquid region and the ratio of volume fraction of liquid phase in the mushy region to porosity (χ/Φ) at $t = 120$ min in the cases with varying C_i and D_b are shown in Figs. 11 and 12, respectively.

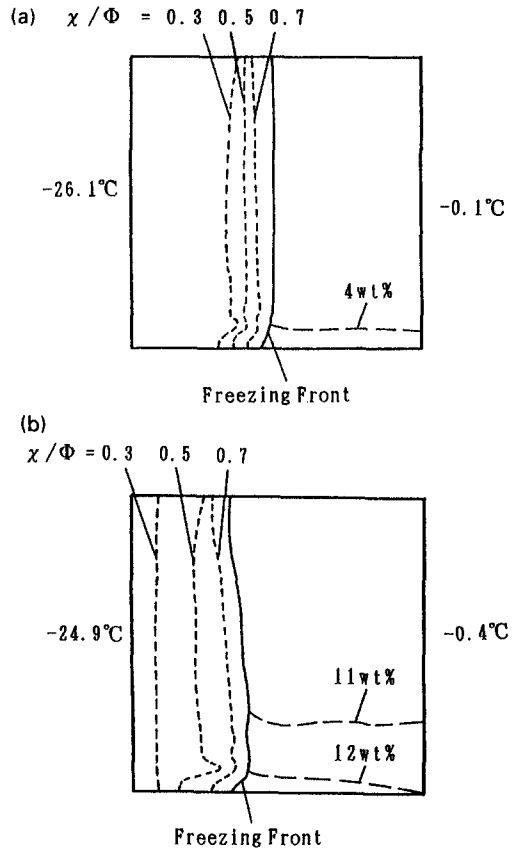

Fig. 11. Analytical results for distributions of concentration in liquid region and (χ/Φ) in the case of vinyl chloride beads. $t = 120$ min, $D_b = 3.76$ mm, $T_i = T_h = 0°C$, $T_B = -30°C$, $\Phi = 0.362$, $k_0 = 7.04 \times 10^{-9}$ m^2. (a) $C_i = 3$ wt% ($Ra_C = -5550$, $Ra_T = 36.9$); (b) $C_i = 10$ wt% ($Ra_C = -4000$, $Ra_T = 29.4$).

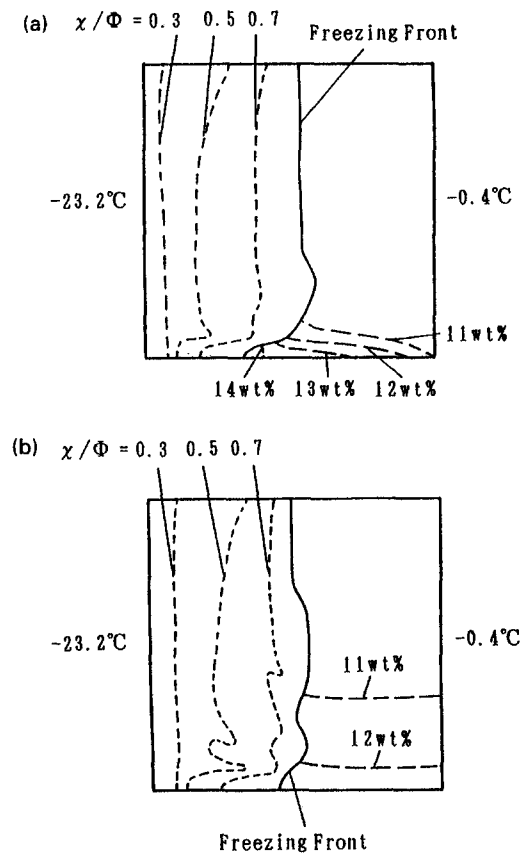

Fig. 12. Analytical results for distributions of concentration in liquid region and (χ/Φ) in the case of glass beads. $t = 120$ min, $C_i = 10$ wt%, $T_i = T_h = 0°C$, $T_B = -30°C$. (a) $D_b = 0.92$ mm ($Ra_C = -97.7$, $Ra_T = 0.717$, $\Phi = 0.380$, $k_0 = 4.73 \times 10^{-10}$ m^2); (b) $D_b = 2.56$ mm ($Ra_C = -1030$, $Ra_T = 7.58$, $\Phi = 0.380$, $k_0 = 5.00 \times 10^{-9}$ m^2).

Corresponding to Fig. 11a and b, the average values of concentration rise in the liquid region were calculated. The average value corresponding to the case of Fig. 11a ($C_i = 3$ wt%) is 0.08 wt% and that corresponding to the case of Fig. 11b ($C_i = 10$ wt%) is 0.59 wt%. The ratio of the former to the latter is about 1/8 (0.08/0.59) and this ratio is smaller than the ratio of the initial concentration in the case of Fig. 11a to that in the case of Fig. 11b (about 1/3). As the value of C_i decreases, the natural convection is suppressed, as shown in Fig. 10 and also the range where (χ/Φ) is relatively large, that is, the range where the natural convection in the mushy region is active becomes narrow. Therefore, when the value of C_i is small, most of rejected solute in the mushy region due to the solidification remains in the mushy region and the solute is hardly transported into the liquid region. Namely, though the solidification range becomes large with the decrease of C_i, the concentration rise in the liquid region becomes small. From the results of Fig. 12a and 12b, the thickness of concentration stratification formed in the liquid region enlarges upward with the increase of D_b. Because the permeability increases with the increase of D_b, so the flow of the solution with high concentration in the mushy region becomes active and the solution easily flows into the liquid region.

Finally, we will discuss the distribution of (χ/Φ). From the comparison of Fig. 11a with b, the range where (χ/Φ) $\geqslant 0.5$, that is, the range where the permeability increases rapidly as shown in Fig. 2, becomes wider with the increase of C_i. As the solidification temperature decreases with the increase of C_i, the heat flux to cool the mushy region decreases, but the value of (χ/Φ) does not decrease. From Fig. 12a and b, it is found that the range where (χ/Φ) $\geqslant 0.5$ becomes wider with the decrease of D_b. Because the convections in the mushy and liquid regions are suppressed with the decrease of D_b, so the growth rate of the freezing front increases and also the rejected solute in the mushy region due to the solidification is hardly transported into the liquid region and remains in the range having the large value of (χ/Φ) near the freezing front. Therefore, in the range where (χ/Φ) in the mushy region is large, the higher concentration of

the solution is kept by the rejected solute and the solidification is suppressed.

5. CONCLUSIONS

The solidification process on a vertical wall of the rectangular cell in which beads saturated with NaCl-aqueous solution were packed was investigated analytically and experimentally. The influences of the mean diameter of beads D_b and the initial concentration of the solution C_i on the solidification process were discussed. The following conclusions were obtained.

(1) For the equation, $(k/k_0) = (\chi/\Phi)^n$, the value of the exponent n increases with the increase of the initial concentration of the solution C_i.

(2) In the case with decreasing initial concentration of the solution C_i:

(i) the natural convection in the liquid region is suppressed;

(ii) the growth rate of the freezing front increases;

(iii) the rate of concentration rise in the liquid region decreases;

(iv) the range of (χ/Φ) where the value of the permeability increases rapidly $[(\chi/\Phi) \geqslant 0.5]$, becomes narrow.

(3) In the case with decreasing the mean diameter of beads D_b:

(i) the natural convections in the liquid and mushy regions are suppressed;

(ii) the growth rate of the freezing front increases;

(iii) the concentration stratifications are formed only near the bottom of the liquid region;

(iv) the range of (χ/Φ) where the value of the permeability increases rapidly $[(\chi/\Phi) \geqslant 0.5]$, becomes wider.

Acknowledgement—The authors wish to thank Mr Nonobe, a former student of Aoyama Gakuin University, for his great co-operation on the experiment.

REFERENCES

1. F. P. Incropera, A. H. H. Engel and W. D. Bennon, Numerical analysis of binary solid–liquid phase change with buoyancy and surface tension driven convection, *Numer. Heat Transfer* Pt A **16,** 407–427 (1989).
2. W. Z. Cao and D. Poulikakos, Freezing of a binary alloy saturating a packed bed of spheres, *J. Thermophys.* **5,** 46–53 (1991).
3. J. Choi and R. Viskanta, Freezing of aqueous sodium chloride solution saturated packed bed from above, *Top. Heat Transfer ASME,* **2,** 159–166 (1992).
4. J. Choi and R. Viskanta, Freezing of aqueous sodium chloride solution saturated packed bed from a vertical wall of a rectangular cavity, *Int. J. Heat Mass Transfer* **36,** 2805–2813 (1993).
5. K. Matsumoto, M. Okada, M. Murakami and Y. Yabushita, Solidification of porous medium saturated with aqueous solution in a rectangular cell, *Int. J. Heat Mass Transfer* **36,** 2869–2880 (1993).
6. H. Rumpf and A. R. Gupte, Einflusse der porositat und korngroßenverteilung im widerstandsgesetz der porenstromung, *Chem. Ing-Techn.* **43,** 367–375 (1971).
7. M. Okada, K. Kimura and I. Watanabe, Analysis of the freezing around a chilled pipe in darcy flow, *Proc. Sixth Int. Heat Transfer Conf.*, Toronto, Vol. 3, EN-6, pp. 31–36 (1978).
8. M. Okada, K. Matsumoto, Y. Yabushita and M. Fukuzaki, Measurement of permeability in a state of solidification of porous medium saturated with solution, *Proc. Third Asian Thermophysical Properties Conf.*, Beijing, pp. 490–497 (1992).